

RESEARCH

Open Access



A massive MIMO-based adaptive multi-stream beamforming scheme for high-speed railway

Yaping Cui* and Xuming Fang

Abstract

The throughput of high-speed railway (HSR) communication systems is limited not only by frequency spectrum but also by high mobility. Under the HSR scenario, one of the promising solutions to improve the throughput is multi-stream beamforming. However, severe performance degradation occurs due to larger inter-beam interference (IBI) as the number of beams is constant. In order to maximize the throughput, a massive multiple input and multiple output (MIMO)-based adaptive multi-stream beamforming scheme is proposed, which utilizes an adaptive beam-selection proposal by exploiting the location information of the train. By adaptively selecting the optimal subset of beams, including active subset size and active receive antenna indices, with respect to the location of the train, the proposed scheme significantly outperforms single/dual-stream beamforming and conventional massive MIMO. We also find that the throughput is not proportional to, but a nonlinear function of, the number of active receive antennas in this scenario.

Keywords: High-speed railway (HSR) communication systems, Massive MIMO, Multi-stream beamforming, Beam selection

1 Introduction

High-speed railway (HSR) communication systems are defined to satisfy the requirements of train-ground data transmission [1]. On the one hand, safety-critical railway signaling (e.g., train control information, security monitoring, and operational services) needs to be transmitted to the ground. On the other hand, the passenger's traveling experience, such as high-rate Internet access, must be supported by more reliable communication quality. Thus, there is practical motivation and interest to investigate how to improve the data rate and transmission reliability of HSR communication systems efficiently to address the different requirements of data transmission.

To fulfill these requirements, several important issues are needed to be investigated, such as serious Doppler effect, synchronization, and frequent handover. Seamless connectivity, soft handover, and fast handover were proposed to provide continuous system connection [2–6]. The timing-frequency training and compressive sensing techniques are used to confirm synchronization [7, 8].

Doppler diversity is one of the most common methods to overcome the Doppler effect [9–11]. The computational complexity can be further reduced by utilizing location and velocity information of the train [12]. In addition, it was proved that the frequency offset estimation and correction are very good in a near constant velocity scenario [13]. Therefore, we assume that the Doppler effect caused by high mobility can be almost compensated by other elaborated solutions. And synchronization can be achieved in the systems.

In this paper, we focus on mitigating the inter-beam interference (IBI) to improve the throughput by utilizing massive multiple input and multiple output (MIMO)-based multi-stream beamforming.

Massive MIMO [14, 15] (also known as large-scale antenna array and very large MIMO) is one of the promising technologies for 5G wireless communication systems, which uses antenna arrays with tens or even hundreds of antennas simultaneously serving many tens of terminals to enhance the system throughput and transmission reliability. Theoretically, as the number of base station (BS) antennas grows without bound, the effects of uncorrelated noise and fast fading disappear [16], the high degree of freedom (DoF) is provided [17], and the distribution of

*Correspondence: cuiyaping321@163.com
Key Laboratory of Information Coding and Transmission, School of Information Science and Technology, Southwest Jiaotong University, 610031 Chengdu, China

the singular values of the channel matrix approaches to a deterministic function [18]. Besides, extra antennas focus energy into a small region [14], which can be helpful to improve the throughput when multi-stream beamforming is employed. Nevertheless, massive MIMO will result in pilot contamination and lower energy efficiency problems [19]. More particularly, performance limitation [20] (i.e., it eventually saturates at a certain value) or degradation [21, 22] can be caused by the transmitters' size.

For HSR, one of the typical terrains is the viaduct (e.g., 86.5% of the Chinese Beijing-Shanghai HSR) [23]. Since the viaduct raises the height of transmit antennas leading to a relatively clear line-of-sight (LOS) and few scatters [24], the benefit of multiple antenna gain is barely harvested. Therefore, there are some limitations to apply massive MIMO to a HSR scenario.

Beamforming can be regarded as forming a signal beam towards the receiver, if there is LOS between the transmitter and receiver. Beamforming can also be applied in non-LOS, if the multipath channel state information (CSI) is known [25]. Several beamforming-based schemes were conceived for HSR communication systems [5, 26–30]. A WiMAX-based route-tracking beamforming was proposed, and field tests over Taiwan HSR were carried out [26]; the experimental results showed that the received signal strength indicator (RSSI), carrier to interference plus noise ratio (CINR), and throughput were improved. In [5, 27–30], location information-assisted opportunistic beamforming, beamforming and location-assisted handover scheme, beamforming and Alamouti STBC combined scheme, location assistant beamforming, and distributed beamforming were proposed to improve system throughput and transmission reliability under HSR scenario by exploiting the regular and predictive location and velocity information of the train. However, in the above schemes, only single-stream beamforming and dual-stream beamforming were adopted but the performance of multi-stream beamforming is not analyzed and discussed in this scenario either.

Based on the above background, multi-stream beamforming is introduced to improve the throughput under HSR scenario. However, performance degradation is caused by the increased IBI with a larger distance between the trackside BS and onboard mobile relay station (MRS) as the number of beams is constant. To overcome the degradation, a massive MIMO-based adaptive multi-stream beamforming (AMSB) scheme is proposed. The proposed scheme is based on an adaptive beam-selection procedure by exploiting the regular and predictive location information provided by train control systems. By adaptively selecting the optimal subset of beams, including active subset size and active receive antenna indices, the maximum throughput has been achieved under HSR scenario.

The rest of this paper is organized as follows. In Section 2, the HSR scenario is presented. Then, in Section 3, the proposed massive MIMO-based AMSB scheme and benchmark conventional massive MIMO are described and analyzed under LOS MIMO channel. Performances of these schemes are evaluated in Section 4. Finally, Section 5 concludes by summarizing the main results and suggests some future work.

2 System model of HSR

Consider that the system model by activating all beams with equal power allocation for HSR communication systems is depicted in Fig. 1. The projection of BS and N_R th receive antenna onto ground are denoted as O and A , respectively. The perpendicular distance between BS and track is d_{\min} . The track-side BS is equipped with uniform linear antenna arrays (ULAA), where the N_T antennas are evenly spaced along a straight line. The transmit antennas are separated by $\Delta_t \lambda_c$, where λ_c is carrier wavelength (e.g., if $f_c = 2.5$ GHz, then $\lambda_c = 0.12$ m) and Δ_t is the normalized transmit antenna separation, normalized to the unit of the carrier wavelength. In addition, the train is moving along the direction of the velocity vector as seen in Fig. 1. The receive antennas of MRS are deployed on the top of each carriage of the train, while the length of the train, l_T , with eight carriages (e.g., CRH-3C train) is used exclusively. The receive antenna separation is $\Delta_r \lambda_c$, where Δ_r is the normalized receive antenna separation. Since the receive antennas are far apart from each other, we assume that the receive antennas are geographically separated [31].

For the sake of mathematical analysis, the distance between BS and reference receive antenna (i.e., the first receive antenna) is denoted as d and the angle between BS and the i th receive antenna is denoted as ϕ_i as seen in Fig. 1. For the sake of simplicity, one data stream per active receive antenna (i.e., the number of beams is equal to the number of active receive antennas) and the number of transmit antennas at BS being not less than the number of receive antennas on the train (i.e. $N_T \geq N_R$) are considered. Furthermore, it is assumed that the CSI can be estimated by the BS due to channel reciprocity in TDD systems [32]; the Doppler shift and channel selectivity caused by high mobility can be almost eliminated by some offset compensation techniques (see, e.g., [9–11, 33–40] and references therein). Many literatures have been devoted to the issues of antenna tracking, training, and synchronization (see [7, 8, 41–44] and the references therein). Therefore, we assume that these problems can be maintained via location prediction and other technologies. Only the downlink is considered in this paper; the uplink will be investigated in our future work. A simple way for the uplink is to activate one or all antennas which is equivalent to the SIMO or MIMO system.

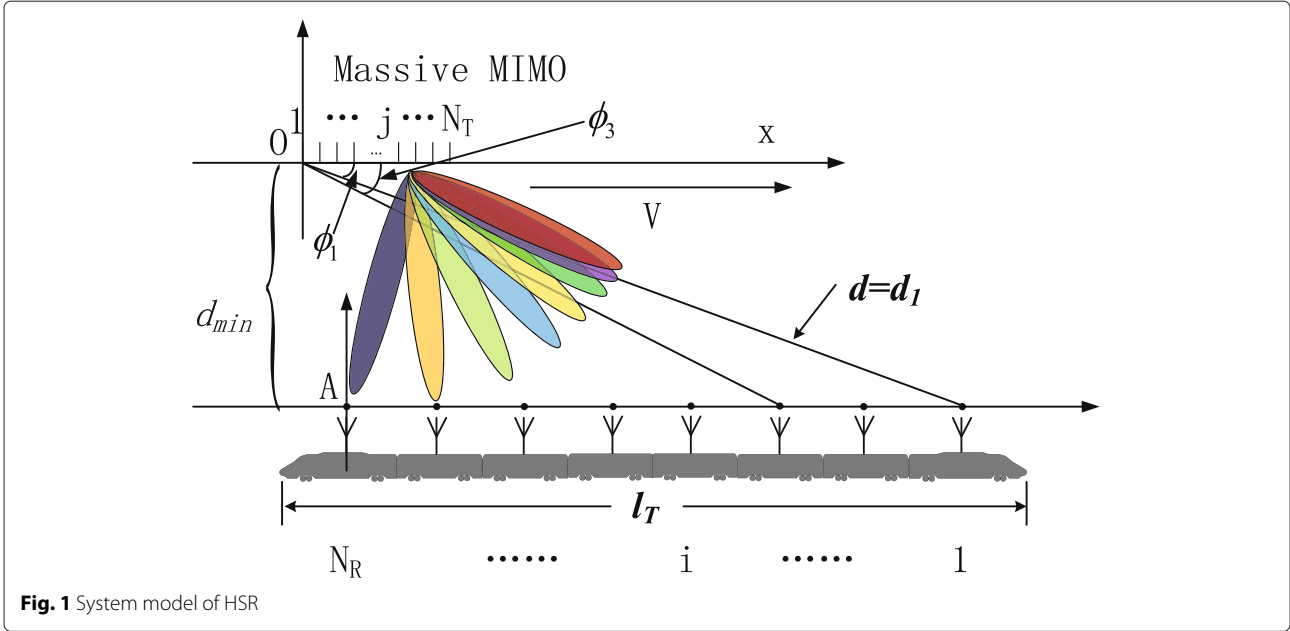


Fig. 1 System model of HSR

According to the system model depicted above, for the multi-stream beamforming with a subset of active receive antennas $\Upsilon \subset \Omega$ (details on the beam-selection procedure given in Section 3), the received signal for i th receive antenna on the train with i th beam can be expressed as:

$$y_i = \sqrt{p_i} \beta_i \mathbf{h}_i \mathbf{w}_i^H x_i + \sum_{j \in \Upsilon, j \neq i} \sqrt{p_j} \beta_j \mathbf{h}_i \mathbf{w}_j^H x_j + n_i \quad (1)$$

where the three terms on the right-hand side of equality represent desired signal, interference signal, and additive white Gaussian noise (AWGN), respectively. p_i is the optimal transmit power for the signal x_i and n_i is independent and identically distributed (i.i.d.) with zero-mean and variance σ_n^2 (i.e., $n_i \sim CN(0, \sigma_n^2)$). β_i is the large-scale fading from the BS to i th receive antenna, which is determined by both path loss and shadowing modeled using the WINNER II D2a [45]. $\mathbf{h}_i = \alpha_i \exp(I2\pi d_i/\lambda_c) \mathbf{f}(\phi_i) \in \mathbb{C}^{1 \times N_T}$ is the small-scale fading [31], d_i is the distance from BS to i th receive antenna (specifically, for the first receive antenna, $d_1 = d$), $\alpha_i \sim N(0, 1)$, $I = \sqrt{-1}$. A simple direction-of-arrival (DoA)-based method is used [46], $\mathbf{w}_i = \frac{1}{\sqrt{N_T}} \mathbf{f}(\phi_i) = \frac{1}{\sqrt{N_T}} [1, e^{-I2\pi \Delta_t \cos \phi_i}, e^{-I2\pi 2\Delta_t \cos \phi_i}, \dots, e^{-I2\pi (N_T-1) \Delta_t \cos \phi_i}] \in \mathbb{C}^{1 \times N_T}$ with power constraint $\sum_{i \in \Upsilon} \|\mathbf{w}_i\|^2 \leq P$, P is the total transmit power of BS, $[\cdot]^H$ denotes Hermitian transportation.

To satisfy the angular resolvability of the receive antenna, the angular separation of any two receive antennas should be of the order of or larger than the length of the transmit antenna array, normalized to the carrier

wavelength [31], i.e., for any $i, j = 1, \dots, N_R, i \neq j$; the angular resolvability requirement is given by:

$$|\cos \phi_i - \cos \phi_j| \geq \frac{1}{N_T \Delta_t} \quad (2)$$

where ϕ_i and ϕ_j represent the directional angles for departure of the path from BS to the i th and j th receive antennas, respectively.

Since $\cos \phi_i$ and $\cos \phi_j$ in (2) can be expressed as:

$$\left\{ \begin{aligned} \cos \phi_i &= \frac{\sqrt{d^2 - d_{\min}^2} + \frac{i-1}{8} l_T}{\sqrt{d_{\min}^2 + \left(\sqrt{d^2 - d_{\min}^2} + \frac{i-1}{8} l_T\right)^2}} \quad (3a) \\ \cos \phi_j &= \frac{\sqrt{d^2 - d_{\min}^2} + \frac{j-1}{8} l_T}{\sqrt{d_{\min}^2 + \left(\sqrt{d^2 - d_{\min}^2} + \frac{j-1}{8} l_T\right)^2}} \quad (3b) \end{aligned} \right.$$

Submitting (3) into (2) yields

$$\left| \frac{\sqrt{d^2 - d_{\min}^2} + \frac{i-1}{8} l_T}{\sqrt{d_{\min}^2 + \left(\sqrt{d^2 - d_{\min}^2} + \frac{i-1}{8} l_T\right)^2}} - \frac{\sqrt{d^2 - d_{\min}^2} + \frac{j-1}{8} l_T}{\sqrt{d_{\min}^2 + \left(\sqrt{d^2 - d_{\min}^2} + \frac{j-1}{8} l_T\right)^2}} \right| \geq \frac{1}{N_T \Delta_t} \quad (4)$$

3 Massive MIMO-based AMSB design and performance analysis of HSR

In this section, a massive MIMO-based adaptive multi-stream beamforming scheme is proposed to maximize the throughput by selecting the optimal subset of beams, including active subset size and active receive antenna indices, under HSR scenario. Then, the benchmark conventional massive MIMO is described briefly.

3.1 Massive MIMO-based adaptive multi-stream beamforming scheme

For the selected subset of active receive antennas, Υ , the corresponding signal to interference plus noise ratio (SINR) for i th beam amounts to:

$$\begin{aligned} \text{SINR}_i &= \frac{p_i \beta_i |\mathbf{h}_i \mathbf{w}_i^H|^2}{\sigma_n^2 + \sum_{j \in \Upsilon, j \neq i} p_j \beta_j |\mathbf{h}_i \mathbf{w}_j^H|^2} \\ &= \frac{p_i \beta_i |\mathbf{h}_i \mathbf{w}_i^H|^2 / \sigma_n^2}{1 + \sum_{j \in \Upsilon, j \neq i} p_j \beta_j |\mathbf{h}_i \mathbf{w}_j^H|^2 / \sigma_n^2} \end{aligned} \tag{5}$$

The optimal p_i in (1) can be found by the waterfilling power allocation policy [47, 48]:

$$p_i = (\mu \lambda_i - 1)^+ \tag{6}$$

where $\lambda_i = 1/\|\mathbf{w}_i\|^2$, $(x)^+ = \max(0, x)$, and μ is the water level satisfying:

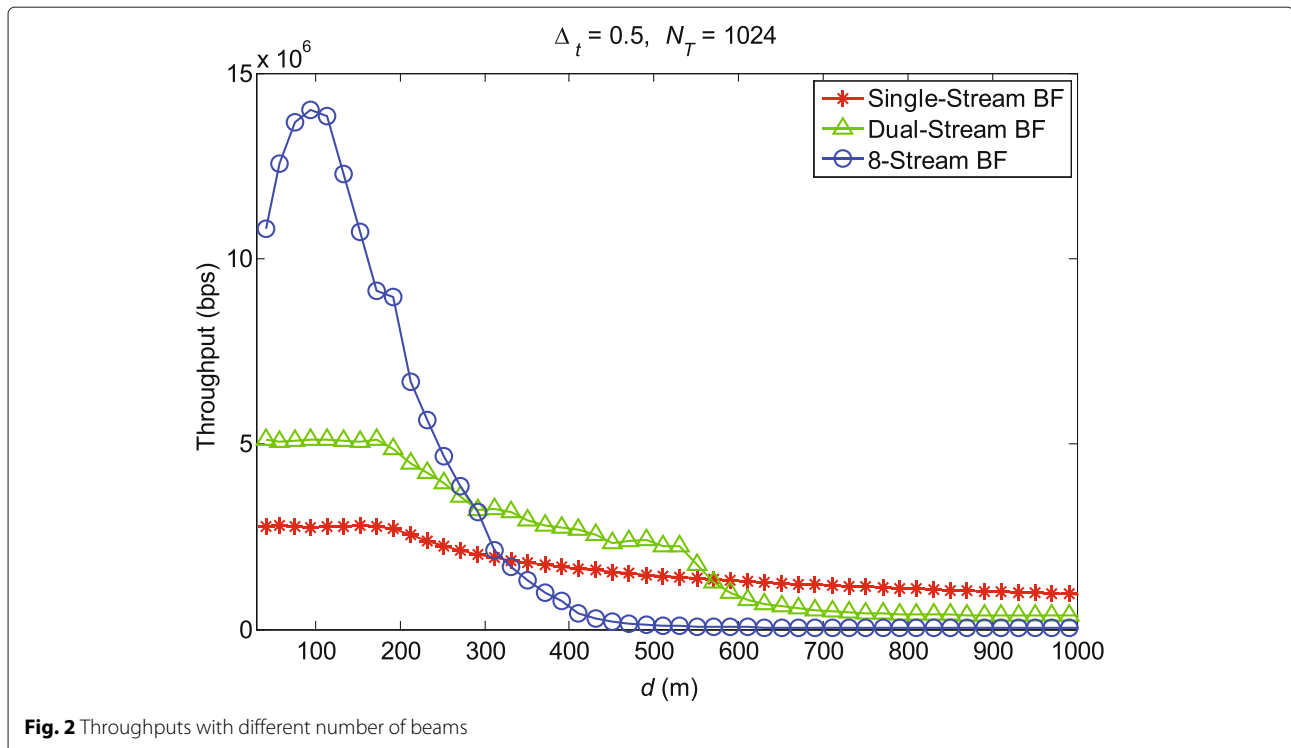
$$\sum_{i \in \Upsilon} (\mu - \lambda_i^{-1})^+ = P \tag{7}$$

Then, the throughput is given by:

$$\begin{aligned} C(\Upsilon) &= E \left\{ \sum_{i \in \Upsilon} B \log_2(1 + \text{SINR}_i) \right\} \\ &= B \times E \left\{ \sum_{i \in \Upsilon} \log_2(1 + \text{SINR}_i) \right\} \end{aligned} \tag{8}$$

where B is the bandwidth and $E[\cdot]$ denotes expectation.

Here, several typical configurations of beamforming are taken as an example. The parameter settings are listed in Table 2 in Section 4 and the performances of single-, dual-, and eight-stream beamforming are shown in Fig. 2. To be specific, the N_R th receive antenna is activated for single-stream beamforming, both first and N_R th receive antennas are activated for dual-stream beamforming, and all receive antennas are activated for eight-stream beamforming. It illustrates that more active beams do not simply mean an increased system performance under HSR scenario (i.e., the throughput is not proportional to the number of active receive antennas), which is bottlenecked by IBI, which is the interference from the other beams sharing the same frequency band. Performance degradation occurs as the number of beams is constant with larger distance between trackside BS and onboard MRS. Thus, to maximize the throughput, the beam-selection procedure is required to determine the optimal subset of beams (i.e., active subset size and active receive antenna indices) with respect to the regular and predictive location of the train.



Based on the above analysis, a massive MIMO-based adaptive multi-stream beamforming scheme is proposed. At the BS, a massive MIMO is used and multi-stream beamforming is introduced. Then, an adaptive beam-selection procedure is applied to select beams. Furthermore, on the top roof of the train, one receive antenna is deployed on each carriage connected by a system bus to a central unit where received signals are processed.

The maximum throughput can be optimized with respect to the selected beam subset Υ . Thus, the beam-selection problem can be formulated as:

$$(P1) \max_{\Upsilon} B \times E \left\{ \sum_{i \in \Upsilon} \log_2(1 + \text{SINR}_i) \right\} \quad (9)$$

s.t.

$$\Upsilon \subset \Omega$$

$$\sum_{i \in \Upsilon} \|\mathbf{w}_i\|^2 \leq P$$

Table 1 Adaptive beam-selection algorithm

Algorithm Adaptive Beam-Selection Algorithm

Initially:

let $n = 1, \Omega = \{1, 2, \dots, N_R\}, \Upsilon = \emptyset$.

$s_1 = \arg \max_{i \in \Omega} P \beta_i |\mathbf{h}_i \mathbf{w}_i^H|^2 / \sigma_n^2$,

$C_{temp} = \max_{i \in \Omega} P \beta_i |\mathbf{h}_i \mathbf{w}_i^H|^2 / \sigma_n^2$,

$\Omega = \Omega - \{s_1\}, \Upsilon = \Upsilon + \{s_1\}$.

Select active receive antenna index:

while $n < N_R$ **do**

$n = n + 1$

for every $i \in \Omega$ **do**

$\tilde{\Upsilon}_i = \Upsilon + \{i\}$

Calculate the total throughput to the active subset $\tilde{\Upsilon}_i$

$C_i =$

$$\sum_{i \in \tilde{\Upsilon}_i} B \log_2 \left(1 + \frac{p_i \beta_i |\mathbf{h}_i \mathbf{w}_i^H|^2 / \sigma_n^2}{1 + \sum_{j \in \tilde{\Upsilon}_i, j \neq i} p_j \beta_j |\mathbf{h}_j \mathbf{w}_j^H|^2 / \sigma_n^2} \right),$$

the waterfilling power allocation is applied according to (6)

$s_n = \arg \max_{i \in \Omega} C_i$

if then $\max_{i \in \Omega} C_i < C_{temp}$

Algorithm terminated. The selected beams subset is Υ .

else

$\Omega = \Omega - \{s_n\}, \Upsilon = \Upsilon + \{s_n\}, C_{temp} = \max_{i \in \Omega} C_i$.

end if

end for

end while

Output:

Υ and C_{temp}

The greedy and discrete stochastic iterative algorithms are commonly used for beam-selection process [49, 50]. However, the greedy algorithm needs to search all possible beam subsets exhaustively, thus leading to high computational complexity. While the discrete iterative algorithm starts by selecting all beams and then performs set reduction. It may result in redundant beams in the selected subset.

Thus, we propose a beam-selection procedure that selects both active subset size and active receive antenna indices with respect to the regular and predictive location of the train to resolve the problem. Let Ω denote the candidate beam subset and Υ denote the selected beam subset. C_{temp} is the maximum system throughput. The proposed procedure is illustrated as follows. Firstly, the single beam with the highest capacity is selected as the initial maximum throughput. And the beam index of the highest capacity is obtained as the initial selected beam subset. Secondly, the beam to maximize the throughput together with the selected beams is found. Then, the algorithm replaces the maximum throughput and updates the selected beam subset. It is terminated when all beams are selected or the throughput drops when more beams are selected. Finally, the algorithm outputs the maximum system throughput and the selected beam subset. The detailed steps are listed in Table 1.

3.2 Conventional massive MIMO scheme

The proposed scheme described in the previous section is based on the massive MIMO technology for 5G. Therefore, the performance of the conventional massive MIMO is used as a benchmark to compare with other techniques. Different from the proposed scheme, conventional massive MIMO activates all transmit/receive antennas simultaneously at transmission and only gets multiplexing gain of the system. The throughput can be expressed as [17, 51]

Table 2 Simulation parameters

Parameter	Value
Bandwidth	10 MHz
Carrier frequency	2.5 GHz
Total transmit power at BS	46 dBm
Number of transmit antennas	1024
Normalized transmit antenna separation	0.5
Radius of the cell	1 km
Distance from BS to track d_{\min}	30 m
Channel model	WINNER II D2a
Length of the train l_T	200 m
Train velocity	350 km/h

$$\begin{aligned}
 C_{\text{MIMO}} &= E_H \left\{ B \log_2 \det \left(\mathbf{I}_{N_R} + \frac{P\boldsymbol{\beta}\mathbf{H}\mathbf{H}^H}{N_T\sigma_n^2} \right) \right\} \\
 &= E \left\{ \sum_{i=1}^{N_R} B \log_2 \left(1 + \frac{P\beta_i \mathbf{h}_i \mathbf{h}_i^H}{N_T\sigma_n^2} \right) \right\} \\
 &= BN_R \times E \left\{ \log_2 \left(1 + \frac{P\beta_i \sum_{j=1}^{N_T} \alpha_j^2 \exp \left(\frac{j4\pi d_i}{\lambda_c} - j4\pi(j-1)\Delta_t \cos \phi_i \right)}{N_T\sigma_n^2} \right) \right\}
 \end{aligned} \tag{10}$$

where \mathbf{I}_{N_R} is the $N_R \times N_R$ identity matrix, $\boldsymbol{\beta} = \text{diag}[\beta_1, \beta_2, \dots, \beta_{N_R}] \in \mathbb{C}^{N_R \times N_R}$ is diagonal matrix, and $\det[\cdot]$ denotes the matrix determinant.

4 Numerical results

The HSR scenario depicted in Fig. 1 is constructed to verify the performance analysis in the previous section. The performance of the proposed scheme is compared to single/dual-stream beamforming and conventional massive MIMO. The detailed values of simulation parameters are listed in Table 2 [45, 52].

Figure 3 illustrates the throughputs of the single/dual-stream beamforming, conventional massive MIMO, and proposed scheme with a different distance between the BS and train as $\Delta_t = 0.5$, $N_T = 1024$. For single-stream beamforming, the N_R th receive antenna is activated. Furthermore, for dual-stream beamforming, both the first and N_R th receive antennas are activated. In contrast to the single/dual-stream beamforming, the throughput of the conventional massive MIMO is strongly influenced by the

location of the train and decreased rapidly when the distance between the BS and train increases. This is because the HSR scenario with the dominance of LOS and few scatters has restricted the multiplexing gain of the MIMO channel. Whereas, the advantages of single/dual-stream beamforming are validated in the LOS environment. The throughputs of single/dual-stream beamforming decrease gradually and do not change drastically, when the distance between the BS and train increases. Meanwhile, the performance of dual-stream beamforming is worse than single-stream beamforming when the influence of IBI becomes more significant as the distance between the BS and train is larger than 570 m. The proposed scheme adjusts the active subset size and active receive antenna indices adaptively with respect to the location of the train. More beams are activated when the train is close to the BS, and fewer beams are activated to reduce IBI when the train is far from the BS. Thus, for the proposed scheme, the maximum throughput has been achieved.

Both the throughput and number of active (selected) beams of the proposed scheme are charted in Fig. 4 with a different distance between the BS and train as $\Delta_t = 0.5$, $N_T = 1024$. It is shown that the optimal number of active beams decreases and degenerates to single-stream beamforming finally when the train travels from the cell center to cell edge and changes periodically when the train travels through the cells. Besides, we also find that the throughput is not proportional to, but a nonlinear function of, the number of active beams, which is bottlenecked by IBI.

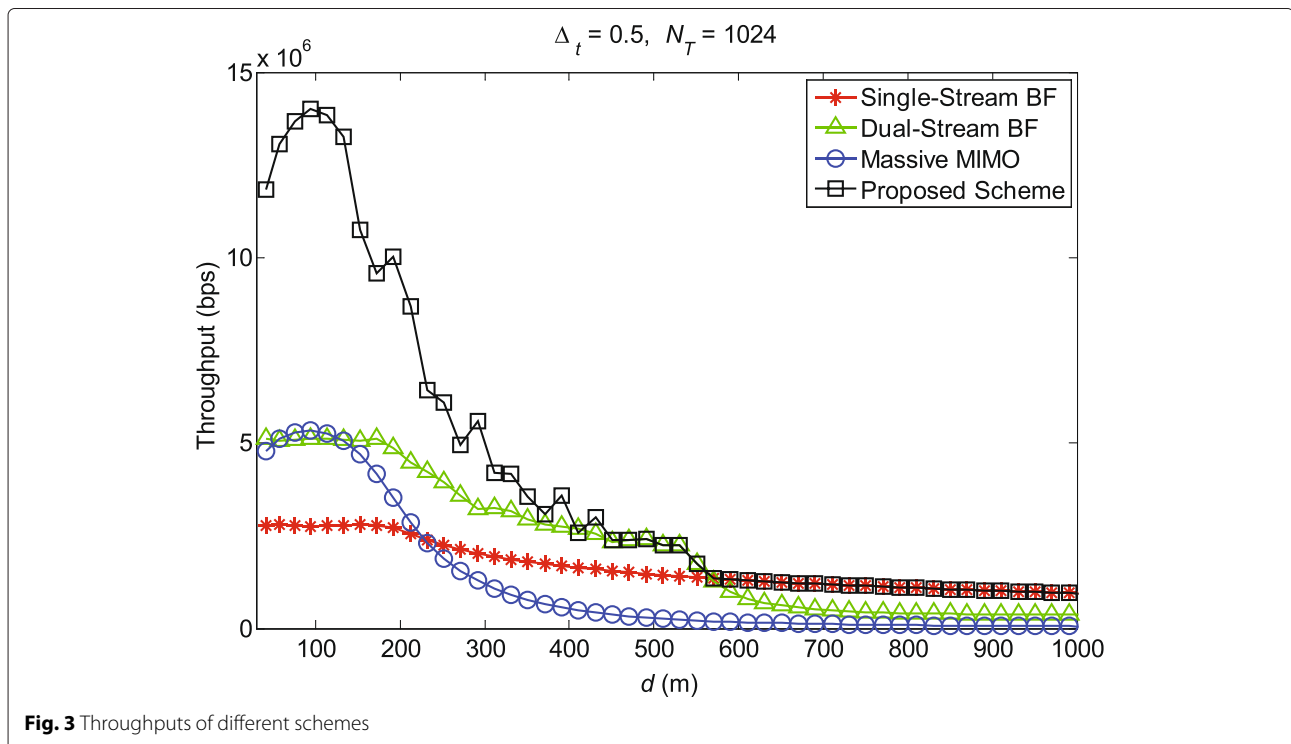
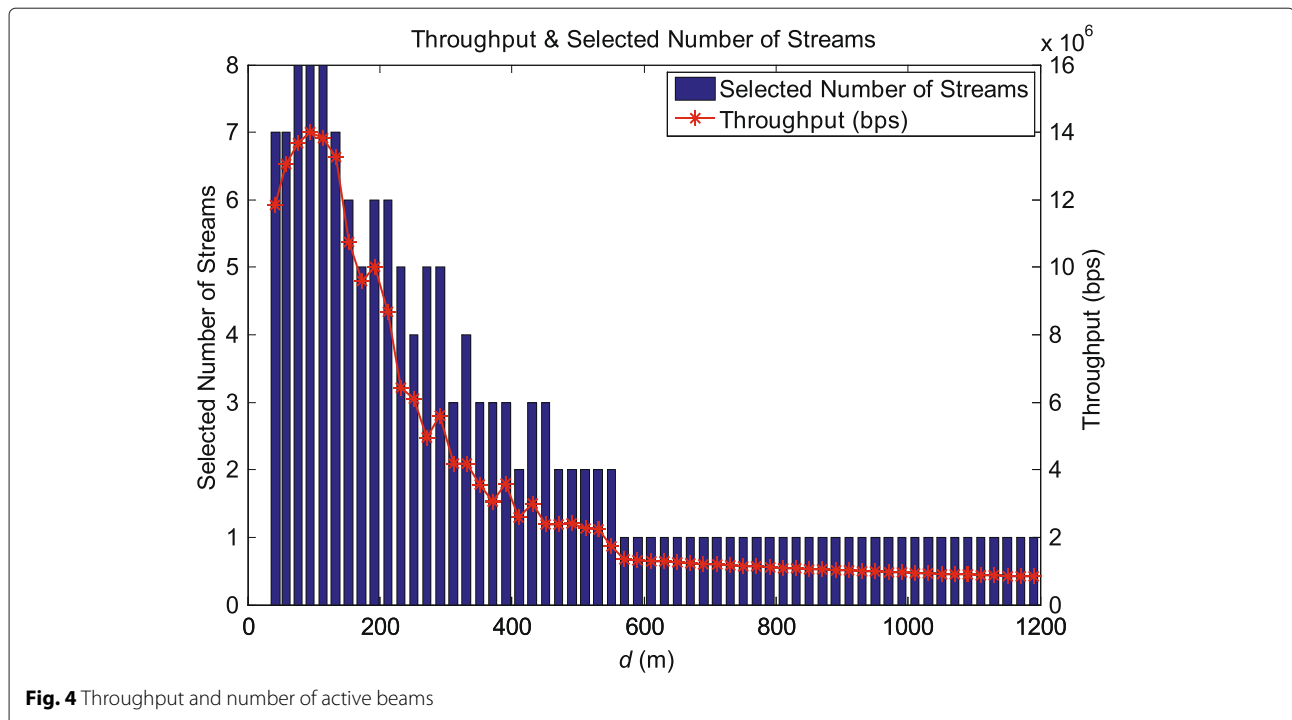


Fig. 3 Throughputs of different schemes



Obviously, the proposed scheme designed in Section 3 maximizes the system throughput.

5 Conclusions

The typical terrain for the HSR scenario is the viaduct in which exists a dominant LOS component. Therefore, the benefit of multiple antenna gain is hardly harvested, and that is one of the challenges for massive MIMO applied under HSR scenario. Although beamforming can form a signal beam towards the given direction which is better than MIMO in a strong LOS environment, the IBI problem of multi-stream beamforming is not yet mitigated. Thus, to maximize the throughput, a massive MIMO-based adaptive multi-stream beamforming scheme is proposed, which selects the active subset size and active receive antenna indices adaptively by exploiting the regular and predictive location information of the train. Numerical results also show that the throughput is not proportional to, but a nonlinear function of, the number of active beams, which is bottlenecked by IBI. Hence, the adaptive beam-selection design is needed in this scenario. Our future work will focus on further research on beam-selection procedure and design a massive MIMO-based multi-stream beamforming scheme for uplink transmission.

Competing interests

Both authors declare that they have no competing interests.

Acknowledgements

This work was supported in part by the 973 Program (no. 2012CB316100), National Natural Science Foundation of China (no. 61471303), and Program for Development of Science and Technology of China Railway Corporation (no. Z2014-X002).

Received: 20 April 2015 Accepted: 3 December 2015

Published online: 12 December 2015

References

- CS Jaime, MG Mariano, IA Jose, FD Alfonso, Long term evolution in high speed railway environments: feasibility and challenges. *Bell Lab. Technical J.* **18**(2), 237–253 (2013)
- OB Karimi, JC Liu, CG Wang, Seamless wireless connectivity for multimedia services in high speed trains. *IEEE J. Select. Areas Commun.* **30**(4), 729–739 (2012)
- MS Pan, TM Lin, WT Chen, An enhanced handover scheme for mobile relays in LTE-A high-speed rail networks. *IEEE Trans. Veh. Technol.* **64**(2), 743–756 (2015)
- YY Xia, XM Fang, WT Luo, M Liu, SS Li, YJ Zhao, Coordinated of multi-point and bi-casting joint soft handover scheme for high-speed rail. *IET Commun.* **8**(14), 2509–2515 (2014)
- M Cheng, XM Fang, WT Luo, Beamforming and positioning-assisted handover scheme for long-term evolution system in high-speed railway. *IET Commun.* **6**(15), 2335–2340 (2012)
- WT Luo, RQ Zhang, XM Fang, A CoMP soft handover scheme for LTE systems in high speed railway. *EURASIP J. Wirel. Commun. Netw.* **2012**(196), 1–9 (2012)
- LL Dai, ZC Wang, ZX Yang, Time-frequency training OFDM with high spectral efficiency and reliable performance in high speed environments. *IEEE J. Select. Areas Commun.* **30**(4), 695–707 (2012)
- LL Dai, ZC Wang, ZX Yang, Compressive sensing based time domain synchronous OFDM transmission for vehicular communications. *IEEE J. Select. Areas Commun.* **31**(9), 460–469 (2013)
- WX Zhou, JX Wu, PZ Fan, High mobility wireless communications with Doppler diversity: fundamental performance limits. *IEEE Trans. Wirel. Commun.* **14**(12), 6981–6992 (2015)

10. WX Zhou, JX Wu, PZ Fan, Energy and spectral efficient Doppler diversity transmissions in high-mobility systems with imperfect channel estimation. *EURASIP J. Wirel. Commun. Netw.* **2015**(140), 1–12 (2015)
11. XQ Luo, ZY Zhang, CJ Zhong, XY Jin, Exploiting cooperative multipath-Doppler diversity in relay-assisted high-speed train communications. *Chin. Sci. Bull.* **59**(35), 5019–5028 (2014)
12. X Ren, W Chen, MX Tao, Position-based compressed channel estimation and pilot design for high-mobility OFDM systems. *IEEE Trans. Veh. Technol.* **64**(5), 1918–1929 (2015)
13. YQ Yang, PY Fan, Doppler frequency offset estimation and diversity reception scheme of high-speed railway with multiple antennas on separated carriage. *J. Mod. Transport.* **20**(4), 227–233 (2012)
14. EG Larsson, O Edfors, F Tufvesson, TL Marzetta, Massive MIMO for next generation wireless systems. *IEEE Commun. Mag.* **52**(2), 186–195 (2014)
15. F Boccardi, RW Heath Jr., A Lozano, TL Marzetta, P Popovski, Five disruptive technology directions for 5G. *IEEE Commun. Mag.* **52**(2), 74–80 (2014)
16. TL Marzetta, Noncooperative cellular wireless with unlimited numbers of base station antennas. *IEEE Trans. Wirel. Commun.* **9**(11), 3590–3600 (2010)
17. F Rusek, D Persson, BK Lau, EG Larsson, TL Marzetta, O Edfors, F Tufvesson, Scaling up MIMO: opportunities and challenges with very large arrays. *IEEE Signal Process. Mag.* **30**(1), 40–60 (2013)
18. AM Tulino, S Verdu, *Random matrix theory and wireless communications*. (Now Publishers, Hanover, 2004)
19. J Hoydis, ST Brink, M Debbah, Massive MIMO in the UL/DL of cellular networks: how many antennas do we need. *IEEE J. Select. Areas Commun.* **31**(2), 160–171 (2013)
20. PD Rahimzadeh, NC Beaulieu, Limits to performance of optimum combining with dense multiple correlated antennas. *IEEE Trans. Commun.* **58**(7), 2014–2022 (2010)
21. S Shen, MR McKay, RD Murch, in *Proc. IEEE ISITA*. MIMO systems with mutual coupling: how many antennas to pack into fixed-length arrays? (IEEE, Taichung, 2010), pp. 531–536
22. C Masouros, M Sellathurai, T Ratnarajah, Large-scale MIMO transmitters in fixed physical spaces: the effect of transmit correlation and mutual coupling. *IEEE Trans. Commun.* **61**(7), 2794–2804 (2013)
23. WT Luo, XM Fang, M Cheng, YJ Zhao, Efficient multiple-group multiple-antenna (MGMA) scheme for high-speed railway viaducts. *IEEE Trans. Veh. Technol.* **62**(6), 2558–2569 (2013)
24. RS He, ZD Zhong, B Ai, GP Wang, JW Ding, AF Molisch, Measurements and analysis of propagation channels in high-speed railway viaducts. *IEEE Trans. Wirel. Commun.* **12**(2), 794–805 (2013)
25. E Bjornson, M Bengtsson, B Ottersten, Optimal multiuser transmit beamforming: a difficult problem with a simple solution structure [lecture notes]. *IEEE Signal Process. Mag.* **31**(4), 142–148 (2014)
26. HH Wang, HA Hou, in *Proc. IEEE PIMRC*. Experimental analysis of beamforming in high-speed railway communication (IEEE, Toronto, 2011), pp. 745–749
27. M Cheng, XM Fang, Location information-assisted opportunistic beamforming in LTE system for high-speed railway. *EURASIP J. Wirel. Commun. Netw.* **2012**(210), 1–7 (2012)
28. M Cheng, XM Fang, L Yan, in *Proc. IEEE WCSP*. Beamforming and Alamouti STBC combined downlink transmission schemes in communication systems for high-speed railway (IEEE, Hangzhou, 2013), pp. 1–6
29. C Wang, RT Xu, J You, ZD Zhong, in *Proc. IEEE IWCMC*. Location assistant beamforming for high speed railway (IEEE, Limassol, 2012), pp. 1108–1112
30. C Wang, RT Xu, ZD Zhong, in *Proc. IEEE ICSP*. Distributed beamforming for high speed railway (IEEE, Beijing, 2012), pp. 1410–1414
31. D Tse, P Viswanath, *Fundamentals of wireless communication*. (Cambridge University Press, Cambridge, 2005)
32. A Adhikary, JY Nam, JY Ahn, G Caire, Joint spatial division and multiplexing-the large-scale array regime. *IEEE Trans. Inf. Theory.* **59**(10), 6441–6463 (2013)
33. O Piirainen, U.S. Patent 6,473,594,29 (2002)
34. TR Banniza, R Klotsche, K Wunstel. U.S. Patent 7,653,347,26 (2010)
35. YQ Yang, PY Fan, YM Huang, in *Proc. IEEE WCSP*. Doppler frequency offsets estimation and diversity reception scheme of high speed railway with multiple antennas on separated carriages (IEEE, Huangshan, 2012), pp. 1–6
36. F Verde, in *Proc. IEEE ISWCS*. Low-complexity time-varying frequency-shift equalization for doubly selective channels (IEEE, Ilmenau, 2013), pp. 1–5
37. I Barhumi, G Leus, M Moonen, Time-varying FIR equalization for doubly selective channels. *IEEE Trans. Wirel. Commun.* **4**(1), 202–214 (2005)
38. F Verde, Frequency-shift zero-forcing time-varying equalization for doubly selective SIMO channels. *EURASIP J. Appl. Signal Process.* **2006**, 245–245 (2006)
39. G Leus, in *Proc. IEEE EUSIPCO*. On the estimation of rapidly time-varying channels (IEEE, Vienna, 2004), pp. 120–123
40. X Meng, JK Tugnait, in *Proc. IEEE ICASSP*. Semi-blind time-varying channel estimation using superimposed training (IEEE, Montreal, 2004), pp. 797–800
41. LMK Timothy, ML Ownby, DG Bowen. U.S. Patent 6,433,736,13 (2002)
42. H Wang, DG Fang, M Li, A single-channel microstrip electronic tracking antenna array with time sequence phase weighting on sub-array. *IEEE Trans. Microwave Theory Tech.* **58**(2), 253–258 (2010)
43. D McAllister, C Ranson, FW Phillips. U.S. Patent 8,681,917,25 (2014)
44. J Lee, H Yu, Y Sung, Beam tracking for interference alignment in time-varying MIMO interference channels: a conjugate-gradient-based approach. *IEEE Trans. Veh. Technol.* **63**(2), 958–964 (2014)
45. J Meinila, P Kyosti, T Jamsa, L Hentila, *Radio technologies and concepts for IMT-advanced*. (Wiley, London, 2009)
46. CA Balanis, *Antenna theory: analysis and design*. (Wiley, New Jersey, 1982)
47. T Yoo, A Goldsmith, On the optimality of multiantenna broadcast scheduling using zero-forcing beamforming. *IEEE J. Select. Areas Commun.* **24**(3), 528–541 (2006)
48. SC Huang, H Yin, HM Li, VCM Leung, Decremental user selection for large-scale multi-user MIMO downlink with zero-forcing beamforming. *IEEE Wirel. Commun. Lett.* **1**(5), 480–483 (2012)
49. M Ding, S Liu, HW Luo, W Chen, MMSE based greedy antenna selection scheme for AF MIMO relay systems. *IEEE Signal Process. Lett.* **17**(5), 433–436 (2010)
50. P Clarke, RC de Lamare, Transmit diversity and relay selection algorithms for multirelay cooperative MIMO systems. *IEEE Trans. Veh. Technol.* **61**(3), 1084–1098 (2012)
51. K Ming, MS Alouini, Capacity of MIMO Rician channels. *IEEE Trans. Wirel. Commun.* **5**(1), 112–122 (2006)
52. G Dalton, *GSM-R Procurement guide*. (UIC Publishing PhysicsWeb, 2007). <http://www.uic.org/>. Accessed February 2007

Submit your manuscript to a SpringerOpen[®] journal and benefit from:

- Convenient online submission
- Rigorous peer review
- Immediate publication on acceptance
- Open access: articles freely available online
- High visibility within the field
- Retaining the copyright to your article

Submit your next manuscript at ► springeropen.com